

free energy of the system. That is, eq A-5 is the boundary condition that represents the effect of  $\gamma$ . After  $q_B(i,j,k,m)$  and  $q_C(i,j,k,m)$  were obtained,  $\rho(i,j,k)$  ( $=\rho(\mathbf{r})$ ) was calculated by eq 5' and 6'. Then the normalization condition for  $\rho(i,j,k)$ , eq 7, was employed, and  $\rho(i,j,k)$  was adjusted by a factor

$$n_B N_m (2N + 1)^3 / D^3 \sum_{\substack{(i,j,k) \text{ in} \\ \text{the matrix} \\ \text{phase}}} \rho(i,j,k)$$

because  $q_K$  is proportional to but not identical with the probability density.

The actual process of obtaining a consistent set of  $q_K$  and  $\rho$  was as follows: First, eq A-2 was solved for  $u = 0$  and the trial functions of  $q_K$  and  $q_C$  were obtained for a given  $\gamma$  by the procedure described above. Then  $\rho$  was calculated from these  $q_B$  and  $q_C$ , and the first trial potential term  $u(i,j,k)$  was calculated from this  $\rho$  by eq 2-4. Then eq A-2 was solved for this  $u(i,j,k)$  and the same steps were repeated until the calculation became convergent. This procedure is similar to the perturbation calculation where the potential term  $u$  acts as an internal disturbance. Thus, the calculation was convergent when the disturbance  $u$  was not very large; i.e., the osmotic compressibility introduced in this term was not very small. When the mean change of  $\rho(i,j,k)$  in the cell and the change of  $Q^*$  (see eq 6') in the subsequent step became smaller than a suitably chosen criterion, say 0.2% of the whole value in this study, the calculation for that  $\gamma$  was terminated, and a new loop for another  $\gamma$  was initiated. Such a calculation sometimes took 2 h or more for five values of  $\gamma$ .

## References and Notes

- (1) Kotaka, T.; White, J. L. *Trans. Soc. Rheol.* **1973**, *17*, 587.
- (2) Masuda, T.; Matsumoto, Y.; Matsumoto, T.; Onogi, S. *Nihon Reoroji Gakkaishi* **1977**, *5*, 135.
- (3) Masuda, T.; Matsumoto, Y.; Matsumoto, T.; Onogi, S. *J. Macromol. Sci., Phys.* **1980**, *B17*, 256.
- (4) Osaki, K.; Kim, B. S.; Kurata, M. *Bull. Inst. Chem. Res., Kyoto Univ.* **1978**, *56*, 56.
- (5) Watanabe, H.; Kotaka, T. *Nihon Reoroji Gakkaishi* **1980**, *8*, 26.
- (6) Kotaka, T.; Watanabe, H. *Nihon Reoroji Gakkaishi* **1982**, *10*, 24.
- (7) Kotaka, T.; Watanabe, H. *Polym. Eng. Rev.*, in press.
- (8) Watanabe, H.; Kotaka, T.; Hashimoto, T.; Shibayama, M.; Kawai, H. *J. Rheol.* **1982**, *26*, 153.
- (9) Watanabe, H.; Kotaka, T. *Polym. J.* **1982**, *14*, 739. The SB samples employed were those with S content less than 30 wt % and molecular weight  $M_n$  less than  $3 \times 10^5$ .
- (10) Shibayama, M.; Hashimoto, T.; Kawai, H. *Macromolecules* **1983**, *16*, 16.
- (11) Meier, D. J. *J. Polym. Sci., Part C* **1969**, *26*, 81.
- (12) Meier, D. J. *Prepr. Polym. Colloq., Soc. Polym. Sci. Jpn.* **1977**, *1*, 83.
- (13) Helfand, E.; Tagami, Y. *J. Chem. Phys.* **1972**, *56*, 3592.
- (14) Helfand, E.; Sapse, A. M. *Ibid.* **1975**, *62*, 1327.
- (15) Helfand, E. *J. Chem. Phys.* **1975**, *62*, 999.
- (16) Helfand, E. *Acc. Chem. Res.* **1975**, *8*, 295.
- (17) Helfand, E. *Macromolecules* **1975**, *8*, 552.
- (18) Helfand, E.; Wasserman, Z. R. *Macromolecules* **1976**, *9*, 879.
- (19) Helfand, E.; Wasserman, Z. R. *Polym. Eng. Sci.* **1977**, *17*, 582.
- (20) Helfand, E.; Wasserman, Z. R. *Macromolecules* **1978**, *11*, 960.
- (21) Hashimoto, T.; Todo, A.; Itoi, H.; Kawai, H. *Macromolecules* **1977**, *10*, 377.
- (22) Hashimoto, T.; Shibayama, M.; Kawai, H. *Ibid.* **1980**, *13*, 1237.
- (23) Noolandi, J.; Hong, K. M. *Ferroelectrics* **1983**, *30*, 117.
- (24) Hong, K. M.; Noolandi, J. *Macromolecules* **1981**, *14*, 727.
- (25) Hong, K. M.; Noolandi, J. *Ibid.* **1981**, *14*, 736.
- (26) Watanabe, H.; Kotaka, T. *J. Rheol.* **1983**, *27*, 223.
- (27) Watanabe, H.; Kotaka, T. *Macromolecules* **1983**, *16*, 769.
- (28) Doi, M., private communication.
- (29) See, for example: de Gennes, P.-G. "Scaling Concepts in Polymer Physics"; Cornell University Press: Ithaca, NY, 1979.
- (30) des Cloizeaux, J. *J. Phys. (Paris)* **1975**, *36*, 281.
- (31) Noda, I.; Kato, N.; Kitano, T.; Nagasawa, M. *Macromolecules* **1981**, *14*, 668.
- (32) Kittel, C. "Introduction to Solid State Physics", 5th ed.; Wiley: New York, 1976.
- (33) Shibayama, M.; Hashimoto, T.; Kawai, H.; Watanabe, H.; Kotaka, T. *Macromolecules* **1983**, *16*, 361.

## Long-Range Order Parameters of Form II of Poly(vinylidene fluoride) and Molecular Motion in the $\alpha_c$ Relaxation

Yasuhiro Takahashi\* and Kazuhiro Miyaji

Faculty of Science, Department of Macromolecular Science, Osaka University, Toyonaka, Osaka 560, Japan. Received January 25, 1983

**ABSTRACT:** Long-range order parameters  $S_A$  and  $S_C$  are defined as linear functions of the structure factor ratios of superlattice spots 120 and 031 to the standard reflection 130, respectively. The reflection intensities of 120, 031, and 130 were measured over the temperature range 55–170 °C by a position-sensitive proportional counter system. The parameter  $S_A$  is independent of temperature, while the parameter  $S_C$  decreases with increasing temperature. This suggests that the reverse motion, which changes the molecular orientation along the fiber axis, takes place in a crystallite. The temperature range corresponds to the  $\alpha_c$  relaxation that is observed, and the reverse motion is essentially the same as that proposed by Miyamoto et al.<sup>6</sup> for the molecular motion in the  $\alpha_c$  relaxation.

The  $\alpha$  relaxation is observed at the highest temperature and the lowest frequency by dielectric measurements of form II of poly(vinylidene fluoride). It was established by several authors<sup>1-3</sup> that the  $\alpha$  relaxation is caused by molecular motion in the crystalline region of form II. Nakagawa and Ishida<sup>4</sup> attributed the  $\alpha$  relaxation to the coupled motion of chain loops at the crystalline surface and chain rotation with a small lengthwise translation in the interior of the crystal. McBrierty et al.<sup>5</sup> interpreted the NMR data by two models: rotation of crystalline chains

in the vicinity of defects and rotational oscillation of restricted amplitude of all chains about the chain axis. Miyamoto et al.<sup>6</sup> proposed a mechanism in which the reverse of the molecular orientation along the fiber axis takes place during movement of a defect region, and Clark et al.<sup>7</sup> characterized the defect region as a solitary wave.

In a previous paper,<sup>8</sup> it was established that in form II crystal, four molecules with different orientation statistically occupy a crystal site with different existence probabilities (Figure 1). The analysis suggests that re-

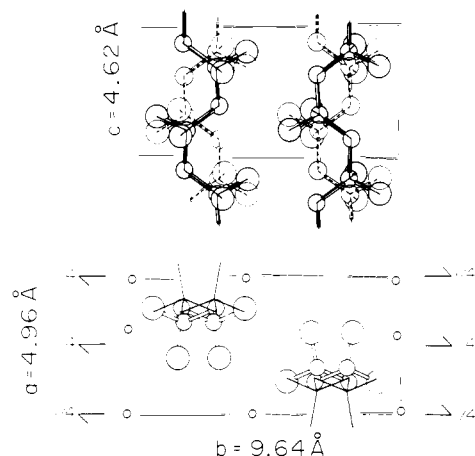


**Figure 1.** Crystal structure of form II of poly(vinylidene fluoride), the sample of which was prepared by annealing at 175 °C for 24 h.<sup>8</sup> The existence probabilities of the molecules with orientations AC,  $\bar{A}\bar{C}$ ,  $\bar{A}C$ , and  $A\bar{C}$  are 54, 29, 10, and 7%, respectively.

flections with  $0kl$ ,  $h + k = 2n + 1$ , correspond to the so-called "superlattice spots", whose intensities decrease to zero since the molecules with different orientation have equal probabilities. Accordingly, it is possible to estimate the quantities of the molecules with different orientation in the crystalline region by measuring the intensities of the superlattice spots.

In the present study, the intensities of the superlattice spots 120 and 031 were measured in the temperature range 55–170 °C, in which the  $\alpha_c$  relaxation is observed, and from the change in the quantities of the molecules with different orientation, the kind of molecular motion that takes place is discussed.

### Experimental Section

Sample KF-1100 (Kureha Chemical Industry Co., Ltd.) was used for poly(vinylidene fluoride). The sample was stretched in a silicone oil bath at 150 °C and was annealed at 175 °C for 24 h after the ends were fixed on a metal holder. X-ray measurements were carried out with Cu K $\alpha$  radiation. The temperature of the sample was controlled within an accuracy of  $\pm 1$  °C by using heating equipment. Intensities of the 120, 130, 031, and 121 reflections were measured by a PSPC (position-sensitive proportional counter) system through heating from 55 to 170 °C. Figure 2 shows the temperature dependence of the intensities.

### Results and Discussion

**Long-Range Order Parameters.** Two long-range order parameters  $S_A$  and  $S_C$  are defined as

$$S_A = 2w_A - 1 \quad (w_A = w_{AC} + w_{\bar{A}\bar{C}})$$

$$S_C = 2w_C - 1 \quad (w_C = w_{AC} + w_{\bar{A}C})$$

where  $w_{AC}$ ,  $w_{\bar{A}\bar{C}}$ ,  $w_{\bar{A}C}$ , and  $w_{A\bar{C}}$  are the existence probabilities of the molecules with orientation AC,  $\bar{A}\bar{C}$ ,  $\bar{A}C$ , and  $A\bar{C}$  at the site of the molecule with orientation AC in the regular structure, respectively (Figure 3). A long-range order parameter is a measure for the regularity of the structure: the long-range order parameter becomes unity when the structure is regular and zero when the structure is completely disordered. The parameter  $S_A$  denotes the measure for the regularity on the  $c$  projection, which becomes zero when the molecules with the orientation A and  $\bar{A}$  statistically coexist with equal probabilities, and the parameter  $S_C$  is the measure for the regularity on the  $a$  projection, which becomes zero when the up (C) and down ( $\bar{C}$ ) molecules coexist with equal probabilities. The long-range order parameters  $S_A$  and  $S_C$  can be linearly related to the structure factors of 120 and 031, respectively. In Figure

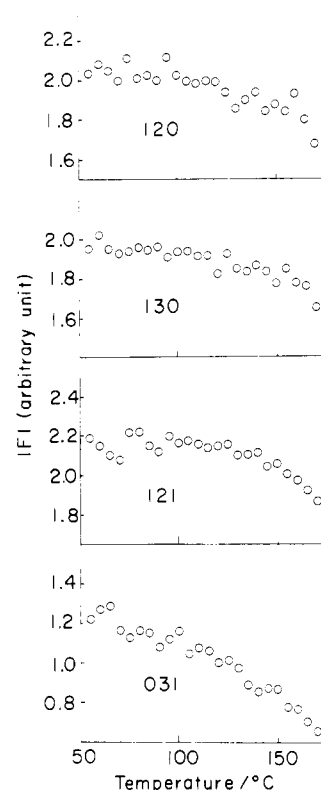


**Figure 2.** Temperature dependence of the structure factors of the reflections 120, 130, 121, and 031.

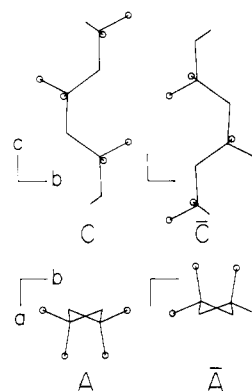


**Figure 3.** Molecular orientation. The symbols A and  $\bar{A}$  denote the molecular orientation on the  $c$  projection and the symbols C and  $\bar{C}$  denote the up and down molecules, respectively. The combinations of the symbols, AC,  $\bar{A}\bar{C}$ ,  $\bar{A}C$ , and  $A\bar{C}$  define the orientation of the molecule.

4, the structure factors of 120 and 031, which are divided by the structure factor of the standard reflection 130 independent of the disorder in order to cancel out the temperature parameter, are plotted vs. the long-range order parameters  $S_A$  and  $S_C$ .

**Structure Change and Molecular Motion.** The temperature dependence of the ratios of the structure factors  $|F_{120}|/|F_{130}|$  and  $|F_{031}|/|F_{130}|$  is shown in Figure 5. The ratio  $|F_{120}|/|F_{130}|$  or  $S_A$  is independent of temperature, while  $|F_{031}|/|F_{130}|$  or  $S_C$  decreases with increasing temperature. In other words, the disorder between molecules with orientation A and  $\bar{A}$  is not affected by temperature and the quantities of molecules with orientation A and  $\bar{A}$  do not change in the crystalline region, while the disorder between up and down molecules becomes larger and the fraction of the up molecule at the up-molecular site in the crystal lattice  $w_C$  decreases with increasing temperature. This suggests that molecules in the crystalline region

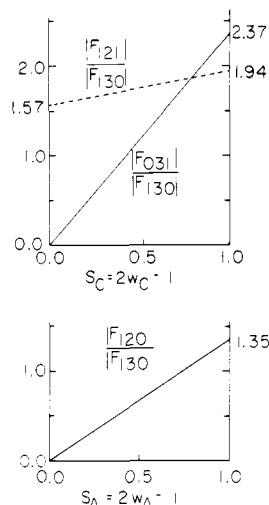


**Figure 4.** Long-range order parameters  $S_A$  and  $S_C$  and the ratios of structure factors  $|F_{120}|/|F_{130}|$ ,  $|F_{031}|/|F_{130}|$ , and  $|F_{121}|/|F_{130}|$ . Here,  $F_{121}$  was calculated on the assumption that only two molecules with orientation AC and AC coexist at a crystal site.

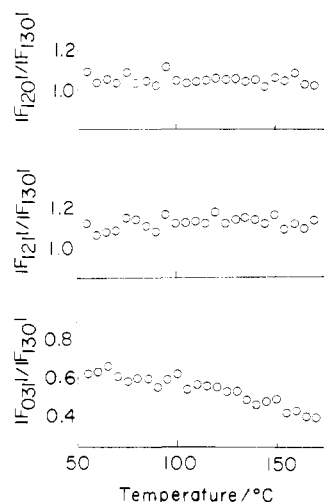


**Figure 5.** Temperature dependence of the ratios of the structure factors,  $|F_{120}|/|F_{130}|$ ,  $|F_{031}|/|F_{130}|$ , and  $|F_{121}|/|F_{130}|$ .

change the orientation up (C) to down ( $\bar{C}$ ) without a change of orientation on the  $c$  projection; that is to say, the molecular motion between up and down, reverse motion, takes place in the temperature range. The reverse motion is caused by the conformational change around the single bond, TGT $\bar{G}$  to GT $\bar{G}$ T (Figure 6). This reverse motion is essentially the same as the motion proposed by Miyamoto et al. for the  $\alpha_c$  relaxation although it cannot be distinguished whether or not the defect region plays any role, and the temperature range 55–170 °C corresponds to the  $\alpha_c$  relaxation that is observed. Furthermore, plots of  $\ln(1 - w_C)/w_C$  vs.  $1/T$  gave  $\Delta H = 2.6$  kJ mol $^{-1}$  and  $\Delta S = 3.0$  J K $^{-1}$  mol $^{-1}$ , which correspond well to  $\Delta G = 0-1.05$  kcal mol $^{-1}$  estimated by dielectric measurement.<sup>6</sup> The value of  $\Delta H$  is consistent with the generally accepted packing energy difference.<sup>9</sup> Therefore, it is concluded that the  $\alpha_c$  relaxation is attributed to the reverse motion of the molecule in the crystalline region. On the other hand, the relation in half-width among a series of reflections, 011, 021, and 031, was interpreted by the antiphase domain structure (Figure 7).<sup>11</sup> From the viewpoint of the packing energy, the molecules in the vicinity of the domain boundary are considered to be less stable than the molecules located in the domain. Accordingly, the reverse motion is reasonably considered to occur among the

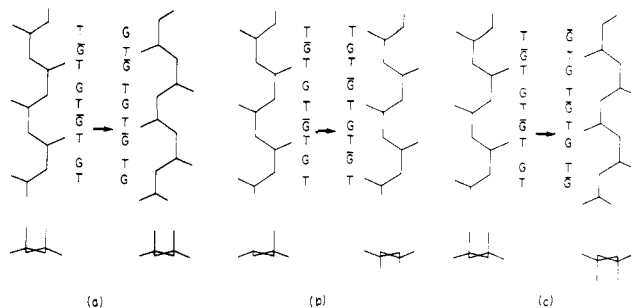


**Figure 6.** Three possible modes of molecular motion in form II: (a) reverse motion, which changes the orientation along the fiber direction; (b) motion that changes the orientation on the  $c$  projection; (c) inversion motion, which changes the orientation simultaneously along the fiber direction and on the  $c$  projection and which is very similar to that found in phase transformation II to III.<sup>10</sup>

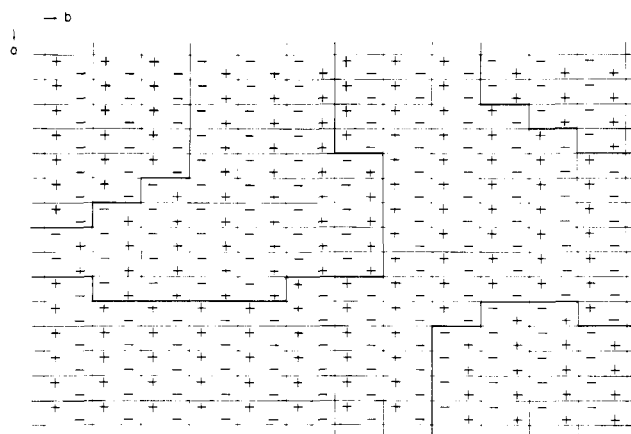


**Figure 7.** Antiphase domain structure for up and down molecules.<sup>9</sup>

molecules in the vicinity of the boundary as if the domain boundary moves.

Here, two other possible factors should be examined, which may bring about the different temperature dependence among the reflections. The first is the anisotropic temperature factor, which is mainly attributed to the different temperature dependence between the vibrational amplitudes perpendicular to and parallel to the fiber axis. However, the ratio  $|F_{121}|/|F_{130}|$  is almost independent of the temperature in the same way as  $|F_{120}|/|F_{130}|$  (Figure 5). This suggests that the temperature dependence of the vibrational amplitude along the fiber axis is at least as large as the one perpendicular to the fiber axis. On the other hand, the ratio  $|F_{121}|/|F_{130}|$  slightly decreases with decreasing  $S_C$  (Figure 4). In spite of the fact that the disorder decreases  $|F_{121}|/|F_{130}|$ ,  $|F_{121}|/|F_{130}|$  is independent of temperature. This suggests that the vibrational amplitude along the fiber axis is less temperature dependent than the one perpendicular to the fiber axis. Accordingly, it is likely that the anisotropy in the vibrational amplitudes rather increases the intensity of the reflection 031. The second possible factor is the partial or surface melting. Generally speaking, it is difficult to consider that the ordered structure melts at a lower temperature than the disordered structure. The antiphase domain structure<sup>11</sup> suggests that the ordered and disordered structures correspond to the major and minor components of the domains in a crystallite, respectively (Figure 7). It is also difficult to consider that the major component of the domains melts at a lower temperature than the minor component.

**Acknowledgment.** We express our sincere thanks to Prof. H. Tadokoro for his constant encouragement and also

to Drs. K. Adachi and H. Ohnuma of this department for their kind discussions.

**Registry No.** Poly(vinylidene fluoride) (homopolymer), 24937-79-9.

## References and Notes

- (1) Sasabe, H.; Saito, S.; Asahina, M.; Kakutani, H. *J. Polym. Sci., Part A-2* **1969**, *7*, 1405.
- (2) Kakutani, H. *J. Polym. Sci., Part A-2* **1970**, *8*, 1177.
- (3) Yano, S. *J. Polym. Sci., Part A-2* **1970**, *8*, 1057.
- (4) Nakagawa, K.; Ishida, Y. *J. Polym. Sci., Polym. Phys. Ed.* **1973**, *11*, 1503.
- (5) McBrierty, V. J.; Douglass, D. C.; Weber, T. A. *J. Polym. Sci., Polym. Phys. Ed.* **1976**, *14*, 1271.
- (6) Miyamoto, Y.; Miyaji, H.; Asai, K. *J. Polym. Sci., Polym. Phys. Ed.* **1980**, *18*, 597.
- (7) Clark, J. D.; Taylor, P. L.; Hopfinger, A. J. *J. Appl. Phys.* **1981**, *52*, 5903.
- (8) Takahashi, Y.; Matsubara, Y.; Tadokoro, H. *Macromolecules*, in press.
- (9) Farmer, B. L.; Hopfinger, A. J.; Lando, J. B. *J. Appl. Phys.* **1972**, *43*, 4293.
- (10) Takahashi, Y.; Matsubara, Y.; Tadokoro, H. *Macromolecules* **1982**, *15*, 334.
- (11) Takahashi, Y.; Tadokoro, H. *Macromolecules*, in press.

# Living Polymerization of $\beta$ -Lactone Catalyzed by (Tetraphenylporphinato)aluminum Chloride. Structure of the Living End

Tomokazu Yasuda, Takuzo Aida, and Shohei Inoue\*

Department of Synthetic Chemistry, Faculty of Engineering, University of Tokyo, Hongo, Bunkyo-ku, Tokyo 113, Japan. Received November 19, 1982

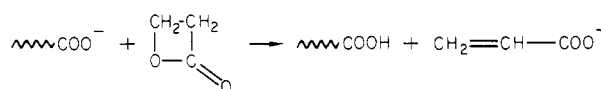
**ABSTRACT:** ( $\alpha,\beta,\gamma,\delta$ -Tetraphenylporphinato)aluminum chloride, obtained by equimolar reaction between diethylaluminum chloride and  $\alpha,\beta,\gamma,\delta$ -tetraphenylporphine, is a good catalyst for the living polymerization of  $\beta$ -propiolactone and  $\beta$ -butyrolactone, to give the corresponding polyesters with narrow molecular weight distribution. By  $^{13}\text{C}$ - and  $^1\text{H}$ -NMR spectrometry, the structure of the living end of the polymer of  $\beta$ -lactone is concluded to be a (porphinato)aluminum carboxylate. The equimolar reaction product between (tetraphenylporphinato)aluminum ethyl and carboxylic acid exhibits a high catalytic activity for the polymerization of  $\beta$ -lactone to form polyester with narrow molecular weight distribution.

## Introduction

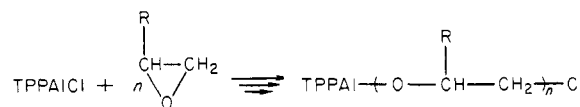
Although the synthesis of polymers of well-controlled molecular weight is of primary importance from both fundamental and practical standpoints, examples up to now have been rather limited. In the polymerization of  $\beta$ -lactone, the proton abstraction reaction from the methylene or methine group adjacent to the carbonyl group of the monomer by propagating species often occurs, resulting in chain transfer, e.g., as shown in Scheme I. The polymerization of  $\alpha,\alpha$ -disubstituted- $\beta$ -lactone has been claimed to be of a living nature on the basis of, e.g., the linear relationship between the molecular weight of the polymer and the conversion of polymerization.<sup>1</sup> More recently, similar behavior has been observed in the polymerization of unsubstituted  $\beta$ -propiolactone catalyzed by alkaline metal acetates coupled with crown ether.<sup>2</sup> However, no direct information as to the molecular weight distribution of the polymers has been described.

We have already reported that ( $\alpha,\beta,\gamma,\delta$ -tetraphenylporphinato)aluminum chloride (TPPAI $\text{Cl}$ ), an equimolar reaction product of  $\alpha,\beta,\gamma,\delta$ -tetraphenylporphine (TPPH $_2$ ) with diethylaluminum chloride ( $\text{Et}_2\text{AlCl}$ ), is an excellent catalyst for the living polymerization of epoxides to give polyethers<sup>3</sup> and their block copolymers<sup>4</sup> with narrow molecular weight distribution. In this polymerization, the propagating end of the living polymer was confirmed to be a (porphinato)aluminum alkoxide (Scheme II).<sup>5</sup> More recently, TPPAI $\text{Cl}$  was found to show a high catalytic activity for the polymerization of  $\beta$ -lactones such as  $\beta$ -propiolactone and  $\beta$ -butyrolactone. The polymerization exhibits a living nature, giving the corresponding polyester having a well-controlled molecular weight with narrow distribution.<sup>6</sup>

Scheme I



Scheme II



In this paper, we report the investigation of the structure of the propagating end of  $\beta$ -lactone in the polymerization catalyzed by TPPAI $\text{Cl}$  in detail, taking advantage of the fact that the propagating end group attached to aluminum may be conveniently observed by NMR analysis because of the signals at high magnetic field due to the large magnetic effect of the porphyrin ring.

## Experimental Section

**Materials.**  $\alpha,\beta,\gamma,\delta$ -Tetraphenylporphine (TPPH $_2$ ) was prepared by reaction between pyrrole and benzaldehyde in propionic acid at about 140 °C and was purified by recrystallization from chloroform-methanol.<sup>7</sup>  $\beta$ -Propiolactone and  $\beta$ -butyrolactone were dried over calcium hydride and then distilled under reduced pressure in a nitrogen atmosphere. Dichloromethane ( $\text{CH}_2\text{Cl}_2$ ) was washed successively with sulfuric acid, water, and aqueous sodium bicarbonate, dried over calcium chloride, and distilled over calcium hydride in a nitrogen atmosphere. Diethylaluminum chloride ( $\text{Et}_2\text{AlCl}$ ) and triethylaluminum ( $\text{Et}_3\text{Al}$ ) were purified by distillation under reduced pressure in a nitrogen atmosphere.

**Measurement.** Gel permeation chromatography (GPC) was performed on a Toyo Soda Model HLC-820UR gel permeation chromatograph equipped with a differential refractometer detector using tetrahydrofuran as the eluent: flow rate, 1.2 mL $\cdot$ min $^{-1}$ ;